ACS APPLIED POLYMER MATERIALS

pubs.acs.org/acsapm

Article

Antimicrobial Cost-Effective Transparent Hydrogel Films from Renewable Gum Karaya/Chitosan Polysaccharides for Modern Wound Dressings

Eva Drápalová, Lenka Michlovská, Hana Poštulková, Ivana Chamradová, Břetislav Lipový, Jakub Holoubek, Lukáš Vacek, Filip Růžička, Markéta Hanslianová, Táňa Svobodová, Eva Černá, Barbara Hrdličková, and Lucy Vojtová*

Cite This: *ACS Appl. Polym. Mater.* 2023, 5, 2774–2786

Read Online

ACCESS | Metrics & More | Article Recommendations | Supporting Information

ABSTRACT: The newest trends in wound healing management and the development of the next generation of dressings are pointing toward natural polymeric materials with important beneficial properties such as antimicrobial effects, renewability, easier process of preparation, and biological activity. Here, we present the preparation and in vitro evaluation of a unique biopolymeric blend composed of natural polymers based on the positively charged polysaccharide chitosan and negatively charged gum karaya. A plate lysis assay of gum karaya and chitosan solution mixtures proved the synergistic antimicrobial effect against specific strains of both Gram-positive and Gram-negative bacteria and yeast. This polymeric mixture was used for hydrogel film preparation and determination of the composition effect on physical properties (swelling behavior in different solvents, pH, diffusion mechanism, hydrolytic stability, mechanical and optical properties). While the pure gum karaya with poly(vinyl alcohol) exhibited the highest hydrolytic degradation (68%), the mixture of poly(vinyl alcohol) and gum karaya with chitosan (in the 25:75 ratio) exhibited the lowest degradation value (41%) due to the strong physical interactions. Cytotoxicity tests performed with hydrogel extracts using two different in vitro models, adherent fibroblasts (NIH3T3) and non-adherent suspension B-lymphocytes (BaF3), exhibited excellent biocompatibility and no cytotoxicity. As expected, the antimicrobial activity of 3-day film extracts showed a significantly improved antimicrobial effect of mixtures involving a chitosan biopolymer. The physical and biological properties of prepared biopolymer-based hydrogels meet the requirements of modern wound dressings.

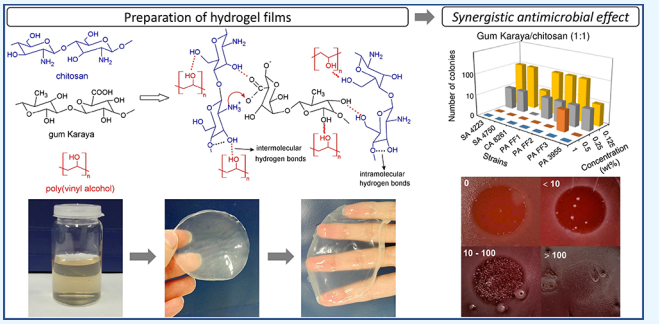

KEYWORDS: *natural gum, polysaccharides, biopolymers, antibacterial activity, cytotoxicity*

1. INTRODUCTION

The application of topical agents is historically the oldest form of treatment for skin injuries, i.e., burns. Records have been preserved from ancient times that show the treatment of burns using different plant materials (resins, honey, vinegar solution, or green tea extract). These plant materials have been used together with dressings. Traditionally, the dressing has been an absorbent permeable cloth such as gauze. The disadvantage of this material is its strong adhesion to the skin, which can present complications during dressing removal (risk of de-epithelization). This can cause trauma to freshly healed wounds; therefore, the regenerative process has to start again.[1,2] Nowadays, many new dressings have been designed and, depending on the type of wound and the cause of the wound, numerous products are available on the market. Modern dressing products come in a wide variety and can be divided into several types—films,[3] foams,[4] composites,[5] sprays,[6] hydrocolloids,[7] gels,[8] and hydrogels,[9] each representing different properties.[1,10] Hydrogels allow moist wound healing and provide optimal conditions for reepithelization (migration, proliferation, and differentiation of epidermal cells), improve fluid balance in the wound bed (exudate or transudate management), and support complete wound closure. Hydrogels are generally obtained from synthetic and natural polymers. Natural polymers are usually starch, cellulose, alginate, dextran, carrageenan, chitin, chitosan (Ch), or gums such as guar gum, gum arabic, or gum karaya (GK). Natural polymers are often mixed with crosslinkers or gel-forming synthetic polymers, such as poly(vinyl alcohol)

Received: January 4, 2023
Accepted: March 22, 2023
Published: April 4, 2023

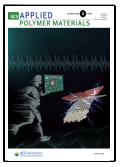

(PVA), which is suitable for producing transparent, flexible, mechanically strong, biocompatible, and cost-effective hydrogel dressings.[11,12] However, pure PVA film does not show antibacterial activity.[13] Natural/synthetic hydrogel mixtures provide unique properties of both materials, especially inherent biocompatibility, biodegradability, and reproducibility with better flexibility and mechanical and antibacterial properties than those of the single components.[10,14−16] Antibacterial wound dressings are very often associated with a certain level of cytotoxicity. High cytotoxicity might delay the healing process by delaying wound closure or promoting local inflammation.[17,18] The potential cytotoxic effect of antimicrobial compounds must be evaluated using relevant in vitro models that mimic the natural microenvironment in vivo as much as possible. As one of the antimicrobial antibacterial compounds, the polysaccharide sterculia gum known as gum karaya can be used. It is a polysaccharide composed of galacturonic acid, β-D-galactose, glucuronic acid, L-rhamnose, and other residues. GK has unique features such as high swelling and water retention capacity[10,19,20] and can be mixed with PVA[20,21] or modified by grafting, crosslinking, carboxymethylation, thiolation, esterification, and interpenetrating polymer networks.[22] Chitosan is a cationic heteropolysaccharide copolymer of *N*-acetyl-D-glucosamine and D-glucosamine consisting of linear β-1,4-linked units. It is characterized by hemostatic effects that help to normalize blood clotting and block nerve endings, resulting in pain reduction, and can be easily processed into hydrogels.[23,24] Chitosan can also form a polymer blend with PVA.[25,26]

The presented study is focused on the preparation of antimicrobial gum karaya−chitosan hydrogels (GK/Ch), natural components, based on the PVA polymer matrix (synthetic component). Hydrogels prepared with different concentrations of GK and chitosan were evaluated in terms of swelling behavior, hydrolytic stability, and biological characterization. The aim was to understand the interactions between the chemical compounds on the molecular level, as well as the interactions between the developed hydrogels and different cell types (prokaryotic and eukaryotic). The antimicrobial effect was studied using the plate lysis assay with selected pathogens. The cytotoxic effect of the selected hydrogels was examined using different assays in two cell lines—NIH3T3 fibroblasts (as an example of adherent cells present in the wound) and BaF3 (precursor B-lymphocytes as an example of non-adherent immune system cells, a model commonly used in the drug discoveries).[27]

2. MATERIALS AND METHODS

2.1. Materials. The gum karaya (commercial-grade, M_w of approx. 9500 kDa), polyvinyl alcohol (M_n = 130 kDa, 99% hydrolyzed), and chitosan with low viscosity (M_w of approx. 250 kDa, degree of deacetylation ≥75%) were purchased from Sigma-Aldrich (Darmstadt, Germany). GK was deacetylated by adjusting the pH to 12 (with 1 M potassium hydroxide (KOH)) and neutralized with 1 M hydrochloric acid (HCl) to pH 7 according to a publication.[20] Sodium hydroxide (NaOH), KOH, HCl, sodium chloride (NaCl), potassium chloride (KCl), potassium dihydrogen phosphate (KH_2PO_4), and sodium dihydrogen phosphate dodecahydrate ($Na_2HPO_4·12H_2O$) were purchased from Lach-Ner (Neratovice, Czech Republic) and used as received. Ultrapure water (Type 1 according to ISO 3696) was prepared using a Millipore purification system (Milli-Q Academic, Millipore, Guyancourt, France). A phosphate-buffered saline solution of pH 7.2 was prepared in a 100 mL volumetric flask of 8 g of NaCl, 0.2 g of KCl, 2.4 g of KH_2PO_4, and 36.3 g of $Na_2HPO_4·12H_2O$. If necessary, the pH was adjusted by adding solutions of NaOH or HCl.

2.2. Antimicrobial Activity Testing. *2.2.1. Bacterial Strains, Culture Conditions, and Sample Preparation.* Bacterial strains based on *Staphylococcus aureus* (SA), *Candida albicans* (CL), and *Pseudomonas aeruginosa* (PA) used in this study are summarized in Table 1. The strains were stored at −70 °C prior to use. Furthermore,

Table 1. Description of Bacterial Strains and Yeast as well as Their Types and Properties

designation	bacterial strain	type	properties
SA 4223	*Staphylococcus aureus*	CCM 4223	methicillin-susceptible
SA 4750		CCM 4750	methicillin-resistant
CL 8261	*Candida albicans*	CCM 8261	(yeast)
PA FF1	*Pseudomonas aeruginosa*	FF 1	multiresistant
PA FF2		FF 2	multiresistant
PA FF3		FF 3	multiresistant
PA 3955		CCM 3955	multiresistant

the bacterial inoculum for a plate lysis assay was prepared in 0.9% NaCl to the density of a McFarland 0.5 turbidity standard from overnight culture in Brain Heart Infusion Broth (Oxoid, UK).

The samples were prepared according to Postulkova et al.[20] and Lipový et al.[28] Deacetylated GK (2% w/v) and chitosan (2% w/v) were dissolved separately in 0.1 M HCl at room temperature and diluted to 1% w/v in 0.9% NaCl. Deacetylated GK (1% w/v), chitosan (1% w/v), and their mixture GK50/Ch50 (1% + 1% w/v) were tested for their antimicrobial properties. A concentration gradient of antimicrobial substances was obtained by serial dilution with normal saline. The final concentration gradient used was as follows: 1, 0.5, 0.25, 0.125, and 0.0625% (all samples % w/v in 0.9% NaCl).

2.2.2. Plate Lysis Assay. Plate lysis assays were measured according to Lipový et al.[28] First, a bacterial inoculum was spread uniformly on blood agar plates, an excess of the bacterial inoculum was removed, and the plates were left to dry for 5 min. Next, 10 μL drops of antimicrobial substances (concentration gradient of GK, chitosan, and their combination) were placed on the surface of the blood agar and then the plates were incubated at 37 °C for 24 h. A NaCl solution (0.9% in water) was used as a growth control. The results were evaluated based on the following growth parameters: total inhibition, i.e., no colonies inside the inhibition zone; substantial inhibition, i.e., <10 colonies inside the inhibition zone; weak inhibition, i.e., >10 and <100 colonies inside the inhibition zone; no visible inhibition zone, i.e., >100 colonies. The tests were performed at least three times in triplicate.

2.3. Preparation of Hydrogel Films. Hydrogels were prepared using a solvent casting method. Deacetylated GK (2% w/v) and chitosan (2% w/v) were dissolved separately in 0.1 M HCl at room temperature, and PVA (2% w/v) was dissolved in water at 100 °C for 4 h. 10 g of PVA solution was added to the vial of a mixture of deacetylated GK and chitosan solution with a defined weight ratio (Table 2). A mixture of polymers was stirred for 4 h at 25 °C to obtain a homogeneous blend and poured into a plastic mold of 30 mm in diameter. All blends were air-dried for 48 h at 25 °C.

2.4. Chemical Characterization of Hydrogel Films. Attenuated total reflection−Fourier transformed infrared spectroscopy was used for the chemical characterization of the prepared hydrogels. Infrared spectra were collected using the Tensor 27 FTIR spectrometer (Bruker, Billerica, USA). Samples were measured in powder form using an ATR with the diamond crystal. The machine was set up to measure the absorbance as a function of the wavenumber between 650 and 3650 cm^{-1}. The number of scans was 32, and the resolution was set to 4 cm^{-1}.

2.5. Swelling Behavior and Hydrolytic Stability. The swelling of the hydrogels as a function of the amount of GK and chitosan was carried out in PBS or water using the gravimetric method according to

https://doi.org/10.1021/acsapm.3c00025
ACS Appl. Polym. Mater. 2023, 5, 2774−2786

Table 2. Hydrogel Films with Different Concentrations of Polysaccharides of the Blend in Dry Matter[a]

sample name	gum karaya (g)	chitosan (g)	PVA (g)	n(GK)/n(Ch)/n(PVA) (mmol)
GK100/Ch0	0.1		0.2	0.684/-/100
GK75/Ch25	0.075	0.025	0.2	0.513/6.5/100
GK50/Ch50	0.05	0.05	0.2	0.342/13/100
GK25/Ch75	0.025	0.75	0.2	0.171/195/100
GK0/Ch100		0.1	0.2	-/260/100

[a]GK—gum karaya, Ch—chitosan, PVA—poly(vinyl alcohol).

ref 29. The hydrogel films were cut into small pieces (approximately 0.02 g in weight and size 1 × 1 cm) and immersed in an excess solvent at a constant temperature (25 °C). The films were removed after 2, 4, 6, 8, 10, 15, 20, 25, 30, 40, 50, 60, 90, and 120 min, and the excess solvent was gently dried with filter paper and immediately weighed. The swelling percentage (%Q) of the hydrogels was calculated using the following equation:

$$\%Q = \left(\frac{W_s - W_d}{W_d}\right)100 \quad (1)$$

where w_s is the weight of swollen hydrogel and w_d is the weight of dried hydrogel film. The swelling of the hydrogel films (GK100/Ch0, GK50/Ch50, and GK0/Ch100) as a function of pH value was carried out in PBS with pH values equal to 2, 4, 6, 8, 10, 12, and 14 at 25 °C after 120 min.

2.6. Determination of the Diffusion Mechanism and Diffusion Coefficient. In the case of water uptake for slabs (in this case for films), the diffusion process is described in eq 2 and is used for the determination of diffusion.[30]

$$M_S = kt^n \quad (2)$$

where M_S is the weight gain, t is time, k is a constant that relates to the structure of the network, and n is a number that determines the type of diffusion. The value n was obtained by plotting the data in log−log plots by using eq 2; the value k was calculated when the value of n was substituted into eq 2. This equation can be applied to a 60% increase in hydrogel mass, i.e., for the initial stages of swelling.

2.7. Hydrolytic Stability. A hydrolytic stability test[31] of the swollen samples was carried out in an incubator at 37 °C in PBS. Hydrogel films with an approximate weight of 0.02 g were left to swell in PBS. After reaching equilibrium in PBS for 24 h, the hydrogels were removed from the vials, blotted dry, and weighed (w_0). The hydrogel films were removed and weighed (w_t) every 15, 30, 45, 60, or 90 days to determine the weight loss. The stability was calculated using eq 3:

$$\text{weight loss } (\%) = 100 - \left(\frac{w_t 100}{w_0}\right) \quad (3)$$

2.8. Mechanical Characterization of Hydrogel Films. The hydrogels' tensile strength and maximum elongation were determined using the RSA-G2 TA rheometer in the hydrated state. The dried hydrogel film was cut into strips (3 × 0.5 cm) and placed between the grips with a 500 μm gap between them. Hydrogel film thickness was determined using a caliper. Hydrogel films were hydrated by immersion in ultrapure water at laboratory temperature for 5 min. Then, the measurement was performed at the constant linear rate set at 0.2 mm·s^{-1} with maximum applied force of 35 N until the sample reached the breaking point. Young's modulus was calculated from the initial slope of the stress−strain curve at the strain of 10%. Samples were analyzed in triplicates and expressed as a mean value ± standard error of the mean. T-test for dependent samples was evaluated with a *p-value <0.05, indicating statistically significant results.

2.9. Optical Properties. The optical transparency of the hydrogel was measured as a light transmittance (%T) in a wavelength range of 400−700 nm using the UV−vis spectrophotometer V-730, JASCO (USA). Hydrogel films were cut into rectangles (20 × 10 mm), dry samples were inserted into quartz cuvettes, and wet samples were hydrated for 5 min before measurement; the air was used as a reference. The transparency was expressed as a transmittance function at 600 nm and light transmittance spectra in the 400−700 nm range.

2.10. In Vitro Cytotoxicity Evaluation of Hydrogel Extracts in Adherent NIH3T3 Cells. NIH3T3 adherent cells were used to evaluate the cytotoxicity of extracts developed from the designed hydrogel films (GK100/Ch0, GK50/Ch50). The tested hydrogel extracts were prepared in 7 mL of NIH3T3 culture medium (10% NCS, 100 U·mL^{-1} of penicillin, 100 μg·mL^{-1} of streptomycin, in DMEM) per well in six-well extract plates with or without sterile dry hydrogels. Empty wells (without hydrogel) containing only the NIH3T3 culture medium were used as a negative control for cytotoxicity. Empty wells with the NIH3T3 culture medium supplemented with 0.2 mg·mL^{-1} sodium dodecyl sulfate (SDS, Sigma-Aldrich, Darmstadt, Germany) were used as a positive control for cytotoxicity. The extract plates were sealed with parafilm to minimize the evaporation of the medium and incubated in a shaker at 100 rpm speed and 37 °C for 72 h. After 72 h of incubation, all extracts were collected from extract plates, pooled together based on the presence or absence of the same hydrogel, and later used for cell treatment.

First, NIH3T3 cells were seeded at a density of 20 × 10^4 cells per well in six-well culture plates in the complete NIH3T3 culture medium and allowed to adhere for 24 h in a humidified cell culture incubator at 37 °C and 5% CO_2. Second, after 24 h of adhesion, the NIH3T3 culture medium was exchanged with previously prepared hydrogel extracts.

NIH3T3 cells were cultured in hydrogel extracts for 24 and 72 h. After each incubation time, cell morphology was examined under the inverted biological bright-field microscope. Furthermore, extracts were aspirated from wells and cells were carefully washed with phosphate-buffered saline (PBS, Sigma-Aldrich, Darmstadt, Germany) to remove non-adherent dead cells that lost their adherence. The living cells attached to the bottom of the wells were stained for 10 min with 0.1% toluidine blue (Sigma-Aldrich, Darmstadt, Germany) in water on an orbital shaker at a speed of 60 rpm at 37 °C. After washing with PBS, the plates were air-dried and macroscopic photos of stained cell layers were taken to visualize the acellular area of dead cells in different hydrogel extracts. Within each experiment, all treatments were performed in triplicate.

2.11. In Vitro Cytotoxicity Evaluation of Hydrogel Extracts on Suspension of BaF3 Cells. A suspension precursor B-lymphocyte cell line BaF3 was used to additionally test the cytotoxicity of the designed hydrogels (GK100/Ch0, GK50/Ch50). BaF3 cells were maintained in a BaF3 culture medium consisting of an RPMI-1640 medium (Biosera, Nuaille, France) supplemented with 10% (v/v) newborn calf serum (NCS, Sigma-Aldrich, Darmstadt, Germany), 4 mM L-glutamine (Biosera, Nuaille, France), 100 U·mL^{-1} of penicillin, 100 μg·mL^{-1} of streptomycin (both Gibco), 600 μg·mL^{-1} of G418 (Sigma Aldrich, Darmstadt, Germany), 50 μM β-mercaptoethanol (Gibco, Sigma-Aldrich, Darmstadt, Germany), and 0.5 ng·mL^{-1} of recombinant mouse interleukin 3 (PeproTech, New Jersey, USA) and cultured in a humidified cell culture incubator at 37 °C and 5% CO_2.

The cytotoxicity assay was performed on BaF3 cells cultured in hydrogel extracts in the six-well plate format. Hydrogel extracts were prepared in 7 mL of the BaF3 basal medium (10% NCS, 4 mM L-glutamine, 100 U·mL^{-1} of penicillin, 100 μg·mL^{-1} of streptomycin, 50 μM β-mercaptoethanol in RPMI-1640) per well in six-well extract plates with or without sterile dry hydrogel. The empty wells (without hydrogel) that contained only the BaF3 culture medium were used as a negative control for cytotoxicity. Empty wells with the BaF3 culture medium supplemented with 0.2 mg·mL^{-1} of SDS were used as a positive control for cytotoxicity. The extract plates were sealed with parafilm to minimize the evaporation of the medium and incubated in

https://doi.org/10.1021/acsapm.3c00025
ACS Appl. Polym. Mater. 2023, 5, 2774−2786

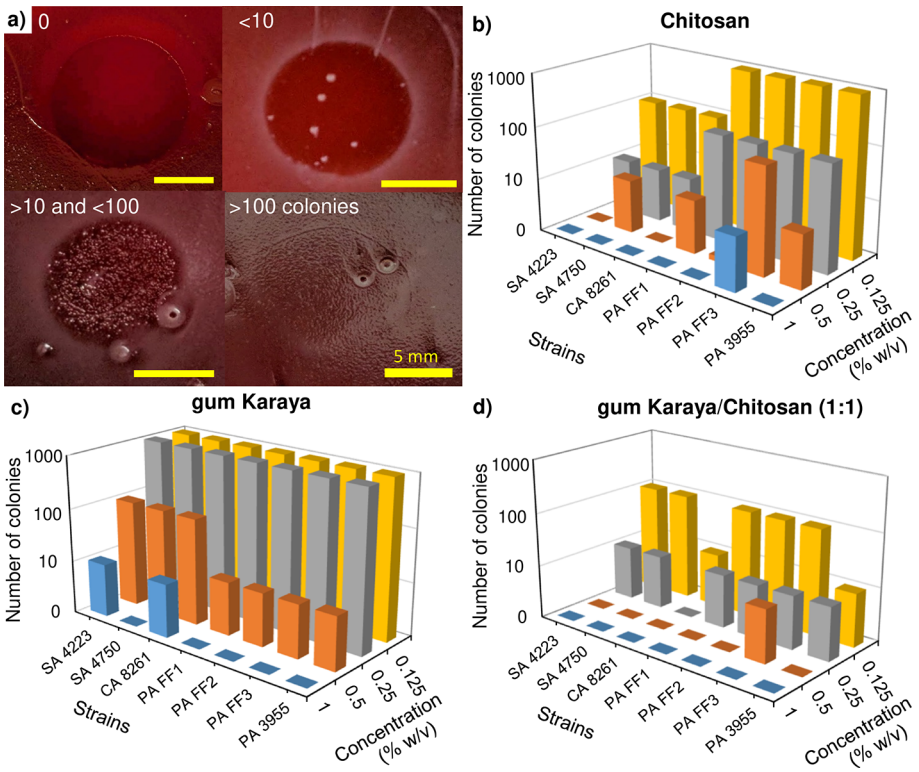

Figure 1. Illustration of test evaluation of antimicrobial activity: (a) 0—total inhibition (no colonies, <10 colonies—substantial inhibition, >10 and <100 colonies—weak inhibition, >100 colonies—no visible inhibition; scale bar 5 mm and results of (b) pure chitosan with different concentrations, (c) pure GK with different concentrations, and (d) gum karaya/chitosan (1:1) with different concentrations.

a shaker at 100 rpm speed and 37 °C for 72 h. After 72 h of incubation, all extracts were collected from the extract plates, pooled together based on the presence or absence of the same hydrogel, and used to seed BaF3 cells with a density of 20×10^4 per well in a total volume of 1.5 mL in new six-well culture plates and incubated at 37 °C and 5% CO_2. Cells were cultured in hydrogel extracts for 24 and 72 h. After each incubation time, cell morphology was examined under the inverted biological microscope.

After 24 h of incubation, the volume of each well was homogenized by pipetting. 20 μL of cell suspension from each well was collected, and cells were manually counted under the microscope in a Bürker hemocytometer chamber using HyClone Trypan Blue Solution (GE Healthcare, Chicago, USA). Dead cells were permeable to the blue dye compared to viable cells with no incorporated dye.

After 24 and 72 h of culture, a resazurin-based proliferation assay was performed to measure cell proliferation in hydrogel extracts. 150 μL (1/10th of the volume of cell suspension per well) of 0.1 mg·mL^{-1} resazurin solution (Sigma-Aldrich, Darmstadt, Germany) in PBS was added to the cells and incubated for 12 h. The addition of resazurin to the medium detects and quantifies cell viability based on the conversion of blue nonfluorescent resazurin dye to red fluorescent resorufin. The fluorescence signal is proportional to the number of living cells. Fluorescence (excitation at 560 nm, emission at 590 nm) was measured using a Synergy H4 Hybrid multimode microplate reader (BioTek, Vermont, USA). Within each experiment, all treatments were performed in triplicate.

2.12. Antimicrobial Activity Testing of Hydrogel Extracts. Bacterial strains used in this study are summarized in Table 1. Extracts were prepared from the designed hydrogel films (GK100/Ch0, GK75/Ch25, GK50/Ch50, GK25/Ch75, GK0/Ch100). Each type of the hydrogel film was incubated in 1 mL of PBS in a shaker at 100 rpm speed and 37 °C for 72 h. PBS alone was used as a negative control. Antimicrobial activity of hydrogel extracts was tested by plate lysis assay described above (Section 2.2.2). Briefly, a bacterial inoculum was spread uniformly on agar plates, an excess of the bacterial inoculum was removed, and the plates were left to dry for 5 min. Next, 10 μL drops of hydrogel extracts were placed on the surface of the blood agar and then the plates were incubated at 37 °C for 24 h. The results were evaluated based on the following growth parameters: total inhibition, i.e., no colonies inside the inhibition zone; substantial inhibition, i.e., <10 colonies inside the inhibition zone; weak inhibition, i.e., >10 and <100 colonies inside the inhibition zone; no visible inhibition zone, i.e., >100 colonies. The tests were performed at least three times in triplicate.

2.13. Statistical Analysis. The statistical analysis of cytotoxic evaluation was performed using GraphPad Prism software (Sant Diego, USA) and one-way analysis of variance (ANOVA test). The level of significance was set as $^*P < 0.05$, $^{**}P < 0.01$, $^{***}P < 0.001$, or $^{****}P < 0.0001$. The bar graphs were generated by SigmaStat 3.5 software (Systat Software, Inc., Bad Friedrichshall, Germany) and show the mean ± SD. Statistical analysis of the tensile strength tests was expressed as a mean value ± standard deviation of the mean. *T*-test for dependent samples was performed in Statistica with $^*P < 0.05$, indicating statistically significant results.

3. RESULTS AND DISCUSSION

In the first part, the bacteriostatic activity of solvents of deacetylated GK, chitosan, and their mixture with different concentrations against strains of *Staphylococcus aureus*, *Pseudomonas aeruginosa*, and *Candida albicans* was evaluated by the plate lysis assay, when a synergistic effect of GK and chitosan mixture was observed. In the second part, hydrogel films based on GK and chitosan with different concentrations and PVA were prepared using a solvent casting method and characterized in terms of both chemical and physical properties. In the last part, in vitro cytotoxicity tests on hydrogel extracts were performed.

3.1. Antibacterial Properties of Gum Karaya, Chitosan, and Their Mixtures. Both the renewable GK[32] and chitosan[33,34] polysaccharides are known to have antibacterial

https://doi.org/10.1021/acsapm.3c00025
ACS Appl. Polym. Mater. 2023, 5, 2774−2786

properties against the growth of several groups of Gram-positive and Gram-negative bacteria and fungi. Ke et al. suggested that Gram-negative bacteria can be more susceptible to chitosan than Gram-positive bacteria.[35] Chitosan, in its polycationic form, shows antimicrobial activity against both Gram-positive and Gram-negative bacteria, acting differently depending on the respective cell membrane structure. In Gram-negative bacteria, chitosan interacts with anionic structures present on their surface, such as lipopolysaccharides and proteins; in Gram-positive bacteria, on the other hand, the chitosan interacts directly with their cell wall layer, consisting of negative charges of peptidoglycan and teichoic acids.[36] For this reason, prior to the hydrogel film preparation, the mutual effect of the combination of GK and chitosan on different bacterial strains was evaluated. The results of the bacteriostatic activity evaluated by the plate lysis assay are summarized in Figure 1. The results were evaluated based on the following growth parameters: total inhibition, i.e., no colonies inside the inhibition zone (Figure 1a, 0); substantial inhibition, i.e., <10 colonies inside the inhibition zone (Figure 1a, <10); weak inhibition, i.e., >10 and <100 colonies inside the inhibition zone (Figure 1a, >10 and <100); no visible inhibition zone, i.e., >100 colonies (Figure 1a, >100 colonies). Chitosan (see Figure 1b) with a concentration of 1% inhibited the growth of all tested microbial strains except the multiresistant strain of *Pseudomonas aeruginosa* FF3, in which less than 10 colonies were observed. Chitosan with 0.5% concentration completely inhibited only methicillin-susceptible *Staphylococcus aureus* CCM 4223, methicillin-resistant *Candida albicans* CCM 8261, and multiresistant *Pseudomonas aeruginosa* FF3. Lower concentrations of chitosan inhibited the growth of all tested microbial strains only weakly or not at all. GK showed lower antimicrobial activity than chitosan alone (Figure 1c). Only at the highest concentration (1%) was GK capable of inhibiting the growth of all *Pseudomonas* strains and *Staphylococcus aureus* CCM 4750. Concentrations less than 0.25% were not able to inhibit bacterial growth in any of the tested strains.

The combination of GK and chitosan (a mixture in a ratio of 1:1) exhibited the best antibacterial results (Figure 1d). The gum karaya/chitosan (1:1) with a concentration of 1% inhibits the growth of all tested microbial strains including methicillin-susceptible, methicillin-resistant, and multiresistant types of bacterial strains. Less than 10 colonies of multiresistant *Pseudomonas aeruginosa* FF3 were observed when 0.5% concentration was used. Other strains showed total inhibition at this concentration. A significant synergistic effect of the chitosan and GK combination can be observed with decreasing concentrations (0.25 and 0.125%), where the antimicrobial properties were improved compared to pure chitosan (Figure 1b) and GK (Figure 1c).

3.2. Characterization of Hydrogel Films by Fourier Transformed Infrared Spectroscopy. Hydrogel films based on GK and chitosan with different concentrations and PVA were prepared using a solvent casting method and characterized by Fourier transformed infrared (FTIR) spectroscopy. The spectra of the hydrogel films are shown in Figure 2. FTIR spectra for individual components (PVA and GK) are interpreted in our previous publications[20] and chitosan in publication.[37] Since the prepared films were not chemically cross-linked and do not contain covalent bonds, mainly physical bonds (hydrogen bonds) were monitored using FTIR spectroscopy similar to what is described in publications.[13,39,38] The absorption band with an intensity at

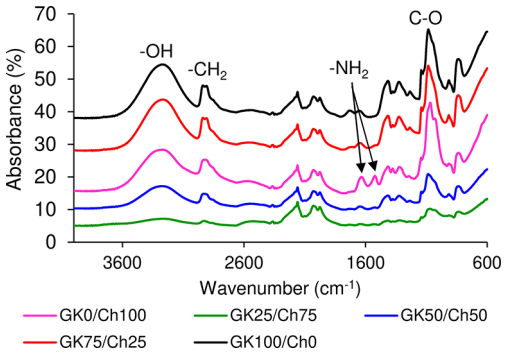

Figure 2. FTIR spectra of gum karaya/chitosan (GK/Ch) blend with different ratios of GK and chitosan.

3250 cm^{-1} represents the −OH stretching vibration of the hydroxy group of PVA, carbohydrate ring of chitosan, and hydroxy and carboxylic groups of GK. All samples contained the same amount of PVA. The intensity of the band at 3250 cm^{-1} decreases with the formation of hydrogen bonds between the hydroxyl group of PVA, chitosan, and GK. We can see higher intensity in hydrogel films from pure GK with PVA. GK has a high molecular weight (approx. 9500 kDa) and does not form hydrogen bonds as easily as in other films where there is only chitosan or a mixture with PVA. The bands at 1645 and 1520 cm^{-1} belong to amide deformation. Lawrie et al.[40] propose that the band at 1520 cm^{-1} corresponds to the N−H bending vibration that overlaps the amide II vibration and that the 1645 cm^{-1} band is for the amide I vibration. The highest intensity of the band is in a film with pure chitosan (GK0/Ch100), whereas in other samples, it decreases due to the formation of ionic interaction between the $-NH_3^+$ and $-COO^-$ groups. The band at 2940 cm^{-1} corresponds to the aliphatic groups of $-CH_2$ in PVA and chitosan. The absorption band of the pyranose ring absorption of GK is between 1180 and 1070 cm^{-1}, amplifying the signal at 1084 cm^{-1} characteristic for C−O stretching of ether groups (C−O−C) in a natural polysaccharide structure. Bands between 2400 and 1850 cm^{-1} belong to the attenuated total reflectance (ATR) crystal (diamond) to which all FTIR spectra were normalized.

3.3. Swelling Behavior. The absorption of solvent into the hydrogel film causes dimensional and physicochemical changes. These changes have been described as a mechanism of polymeric swelling. Swelling at 25 °C was studied as a function of the amount of both GK and chitosan polysaccharides in both PBS with a pH equal to 7.2 and distilled water with a pH equal to 6.5. The effect of different pH values of the solvent on the swelling behavior of polymer blends was evaluated. All samples contained the same amount of PVA as a matrix; only the ratios between GK and chitosan were changed.

The diffusion mechanism is based on the relative rates of water diffusion and polymer relaxation, and accordingly, the mechanism is determined by the classification of diffusion. Case I (or simple Fickian diffusion) occurs when the rate of diffusion is much less than the relaxation rate. Anomalous diffusion (or non-Fickian) occurs when the diffusion and relaxation rates are comparable; the value of n is between 0.5 and 1.0. Case II occurs when diffusion is very rapid compared to the relaxation process; the value of n = 1.0, and the system is controlled by relaxation.[41−43] The diffusion exponent n and the

https://doi.org/10.1021/acsapm.3c00025
ACS Appl. Polym. Mater. 2023, 5, 2774−2786

characteristic of the gel k were evaluated for all polymer blends to determine the mechanism of the swelling kinetics.

3.3.1. Swelling Behavior as a Function of the Hydrogel Film Composition. The swelling behavior of the hydrogel films in PBS was highly dependent on their compositions, as shown in Figure 3. The samples reached maximum swelling in 10 min.

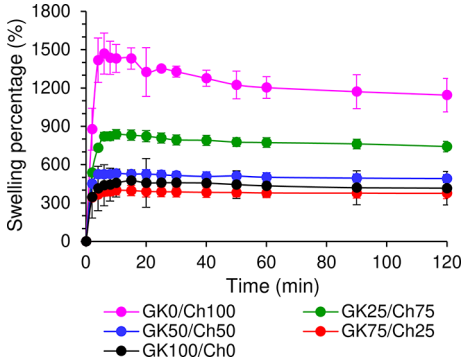

Figure 3. Swelling behavior of the gum karaya/chitosan (GK/Ch) blend with different ratios of GK and chitosan in PBS at 25 °C. Measurements were performed three times for each sample.

The GK0/Ch100 hydrogel film was the most hydrophilic due to the high amount of hydroxyl groups (−OH) and 2-hydroxymethyl groups (−CH_2−OH). These groups were in proximity and hydrated upon contact with PBS. This aspect leads to the possibility of absorbing a large amount of PBS solution up to 1470 ± 160% in the first 6 min. In the case of the GK0/Ch100 hydrogel film, the hydrogen bonds disintegrated rapidly and the water content decreased to 1145 ± 130% in 2 h. The water uptake of the GK25/Ch75 hydrogel films (green line in the graph) reached a maximum value of 840 ± 100%. Besides the hydrogen bonds among hydroxyl groups in chitosan, GK, and PVA, ionic interactions occurred between protonated amino groups (−NH_3^+) in chitosan and the deprotonated carboxylate group (−COO^-) in GK. These ionic interactions are stronger than hydrogen bonds, so the swelling of the GK25/Ch75 hydrogel was about 73% lower compared to the GK0/Ch100 hydrogel. This trend is also copied by GK50/Ch50 hydrogels with a maximum swelling percentage of 530 ± 20% (50% decrease compared to GK0/Ch100) and GK75/Ch25 with a maximum swelling percentage of 400 ± 40% (lowest value). The pure GK hydrogel film GK100/Ch0 and PVA with intermolecular hydrogen bonds had a minimum swelling percentage equal to 480 ± 80%. With a deviation, this is comparable to the GK75/Ch25 sample.

3.3.2. Swelling Behavior as a Function of the Type of Solvent. The swelling of polymer blends containing GK and chitosan in different ratios but with the same amount of PVA was studied in both PBS and distilled water. Swelling was different for different ratios between GK and chitosan and also for the swelling medium, as shown in Figure 4a. Samples containing pure chitosan (GK0/Ch100) and PVA exhibited a higher swelling in distilled water than in PBS. Chitosan together with water-soluble PVA contains hydrophilic groups (−OH, −NH_2) and leads to an increased swelling in distilled water (1144 ± 365%). Chitosan with a pKa of 6.3 is positively charged (−NH_3^+) in water (pH = 5.5) and forms ionic bonds. PVA is physically entangled by intermolecular hydrogen bonds with chitosan and GK −OH groups. The increasing amount of GK and the decreasing amount of chitosan decrease the swelling of water and PBS. GK contains carboxylic acid groups −COOH, which are protonated under acidic conditions, and these groups form salts in the PBS medium. Hydrogel films containing fewer hydrophilic groups from chitosan exhibited reduced swelling.

There were no significant differences among samples GK50/Ch50, GK75/Ch25, and GK100/Ch0. The minimum value of swelling for sample GK100/Ch0 was 417 ± 15% and 308 ± 11% in the PBS and water, respectively. The lower swelling for the higher amount of GK in the water is due to the interaction between −COOH groups and hydrogen bonds, which forms a physical network between polymers, and this network is interrupted by adding ions to the PBS medium (Figure 4b,c).[40,44]

3.3.3. Diffusion Mechanism and Diffusion Coefficient. The values of the diffusion exponent n and gel characteristic constant k for the swelling of polymer blends in PBS have been evaluated from the slope and intercept of the plot of ln M_t/

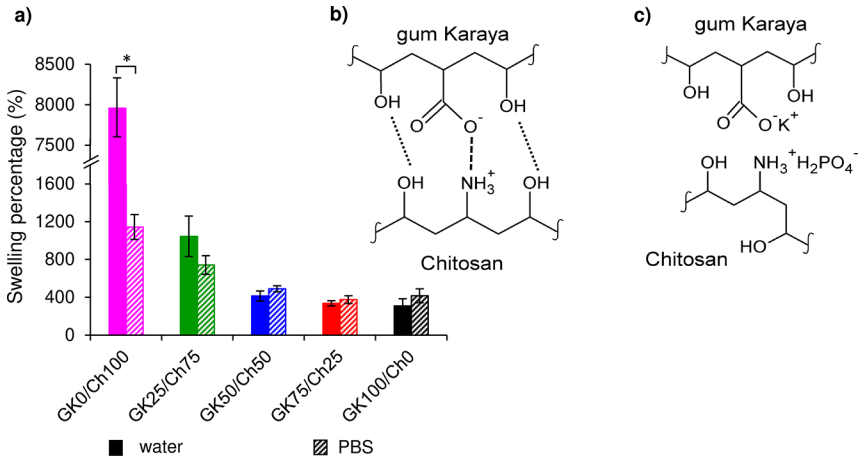

Figure 4. (a) Swelling percentage of hydrogel films of gum karaya/chitosan (GK/Ch) blend with different ratios of GK and chitosan in water (fully) and PBS (oblique stripes) at 25 °C after 120 min, * significance ($P < 0.05$). Measurements were performed three times for each sample. Schemes of (b) electrostatic and hydrogen interactions between GK and chitosan in distilled water (pH 5.5), where dotted lines represent hydrogen bonds between −OH groups and the dashed line the electrostatic interaction between −COO^- and −NH_3^+, and (c) the screening effect of counterion in the PBS medium (pH 7.2).

https://doi.org/10.1021/acsapm.3c00025
ACS Appl. Polym. Mater. 2023, 5, 2774−2786

M_{max} versus ln t, and the results are presented in Figure S1 in the Supporting Information. All results are summarized in Table 3.

Table 3. Results of Diffusion Exponent n, the Characteristic Constant of Gel k, and Various Diffusion Coefficients for the Swelling Kinetics of the Gum Karaya/Chitosan (GK/Ch) Hydrogels at 37 °C

sample name	diffusion exponent n	gel characteristic constant$k \times 10^2$	diffusion coefficient $D \times 10^4$ ($cm^2 \cdot min^{-1}$)
Effect of amount of GK and chitosan			
GK100/Ch0	0.48	1.62	4.90
GK75/Ch25	0.58	1.05	6.09
GK50/Ch50	1.08	0.66	7.86
GK25/Ch75	1.10	0.44	17.25
GK0/Ch100	2.05	0.12	17.90
Effect of pH (GK50/Ch50)			
distilled water (pH = 5.5)	0.44	2.42	3.48
PBS (pH = 7.2)	1.08	0.44	6.09

The diffusion exponent decreased with an increasing amount of GK in GK/Ch blends together with the diffusion coefficient. This is due to the increasing amount of GK, which forms many hydrogen bonds between itself and the PVA matrix. Samples containing only GK and the PVA matrix (GK100/Ch0) had a diffusion exponent equal to 0.48 and indicated the Fickian diffusion mechanism. On the other hand, the diffusion exponent and the diffusion coefficient increased with the increasing amount of chitosan. This is due to the presence of hydrophilic groups ($-NH_2$, primary $-OH$) in the chitosan structure. It allows faster diffusion of solvent molecules into the hydrogel compared to the relaxation process, and the system is controlled by the relaxation rate. The relaxation rate is closely related to the migration of liquids inside the network, which has an impact on the faster migration of active pharmaceutical substances to damage the tissue or debridement of the wound.[31−33]

3.3.4. Swelling of Gum Karaya, Chitosan, and Polyvinyl Alcohol Blends as a Function of pH. During the treatment of the infection, the pH in the wound changes. A wound infection can present a pH up to 10.0 due to the presence of different bacterial strains.[44] The acidic pH of the skin is one of the key mechanisms that protect it from microbial infections. In wounds, an increasing alkaline pH is a predictor of whether they will become nonhealing or chronic.[45] For this reason, we monitored the influence of pH on the swelling of prepared films. The ionic interactions between GK, chitosan, and PVA displayed pH-sensitive swelling. The influence of different pH values (ranging from 2 to 12) on swelling behavior was studied (Figure 5a). The GK0/Ch100 sample involving only chitosan and PVA showed a higher swelling percentage at a lower pH (333% at pH ∼ 2 versus 305% at pH ∼ 4) due to electrostatic repulsion between protonated $-NH_2$ leading to chain expansion, which allows easier diffusion and higher water absorption of the hydrogel films.[46,47] On the contrary, the GK100/Ch0 sample containing only GK and PVA exhibited higher swelling percentage values at a higher pH (324% at pH ∼ 12 vs 246% at pH ∼ 10) due to the electrostatic repulsion between $-COONa$ groups. The GK50/Ch50 sample obtained by both GK and chitosan achieved the highest swelling at pH ∼ 8 (Figure 5a) due to the pKa values of each polysaccharide. In general, carboxylic acids in the GK structure are connected to a value of pKa of around 4.7, while amino groups in the chitosan structure have a value of pKa ∼ 6.5. Under acidic conditions (pH ∼ 3), swelling behaviors are controlled by amino groups of chitosan that are protonated, causing the swelling increase. If the pH value is very low (pH < 3), the screening effect of the counterion (Cl^-, $H_2PO_4^-$) shields the $-NH_3^+$ groups, which does not allow the effective repulsion between protonated amino groups, and thus results in the decrease in swelling. At pH > 4.7, the carboxylic acid groups are ionized due to their pKa value. Above pH 4.7 but below pH 6.4 (and in a certain pH range from 4 to 7), the base groups exist as $-NH_3^+$ and acid groups as $-COO^-$ or as $-NH_2$ and $-COOH$. In the first case, the ionic interactions between $-NH_3^+$ and $-COO^-$ lead to ionic crosslinking. In the second case, hydrogen interactions between $-NH_2$ and $-COOH$ can lead to decreased swelling. At a higher pH value (pH ∼ 8), the carboxylic acid groups become ionized and electrostatic repulsion prevails, causing swelling enhancement. At pH values higher than 10, the screening effect of counterions (Na^+, K^+, Ca^{2+}) shields $-COO^-$ groups from electrostatic repulsion while reducing swelling.[30,32,48,49] The scheme of the influence of pH on physical behavior is shown graphically in Figure 5b.

3.4. Erosion at Simulated Physiological Conditions. Erosion of the samples was performed in PBS at 37 °C for 90 days to mimic the physiological conditions of the human body. Samples containing both GK and chitosan eroded more slowly than samples that had only one of them (Figure 6). This is due to the interactions between carboxylic acid groups from GK and amino groups from chitosan. PBS with pH ∼ 7.4 caused

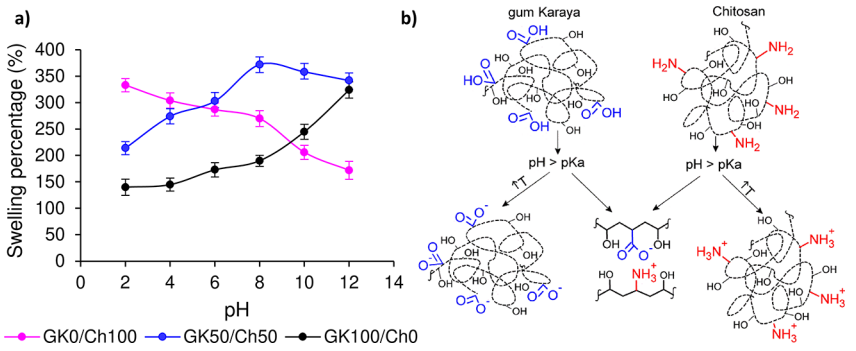

Figure 5. Comparison of swelling behavior of gum karaya/chitosan (GK/Ch) hydrogel (GK0/Ch100, GK50/Ch50, and GK100/Ch0) at different pH levels (a). Influence of pH on physical behavior (b).

https://doi.org/10.1021/acsapm.3c00025
ACS Appl. Polym. Mater. 2023, 5, 2774−2786

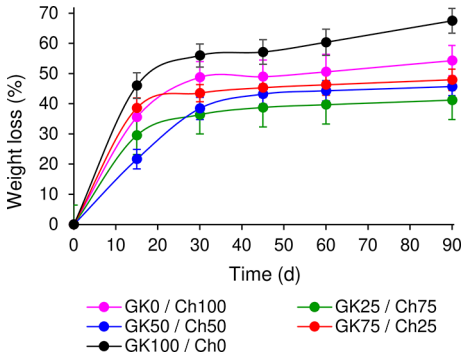

Figure 6. Erosion of gum karaya/chitosan (GK/Ch) films with different ratios of GK and chitosan in PBS at 37 °C.

partial ionization of carboxylic acid groups to −COO− while some amino groups were in the form $-NH_3^+$.[50,51] Interactions between $-NH_3^+$ and $-COO^-$ led to a reduction in swelling. Furthermore, some carboxylic acid groups stayed protonated to −COOH and some amino groups remained as $-NH_2$, allowing for hydrogen interactions. The lowest weight loss value was observed for sample GK25/Ch75 (41% weight loss), while the highest (68%) showed the reference sample of pure GK and PVA (GK100/Ch0) due to the solvation of the carboxylic acid group to −COONa, leading to repulsive forces between these groups and enabling better penetration of the PBS into the hydrogel.

Scheme 1 shows the proposed mechanisms inspired by publications[52,53] and based on FTIR results (Section 2.4) for the reaction of chitosan, GK (both dissolved in 1 M HCl), and PVA aqueous solution. The solutions were mixed at 25 °C for 4 h. In the first step, physical crosslinking was observed by ionic interaction between protonated amino groups ($-NH_3^+$) in chitosan and the deprotonated carboxylate group ($-COO^-$) in GK. PVA reacted with both GK and chitosan through intermolecular hydrogen bonds. At the same time, intramolecular hydrogen bonds arose in the chitosan chains.

3.5. Adhesion Test of Adherent NIH3T3 Cells on the Hydrogel Surface. Adherent NIH3T3 cells were used to study the adhesion of fibroblasts to the selected hydrogels (GK100/Ch0, GK50/Ch50) to mimic the situation in which a hydrogel wound dressing would be placed on the surface of the open wound skin. Using light microscopy, no cells were observed on the hydrogel surfaces of GK100/Ch0 and GK50/Ch50 (Figure 7a,b), which suggests a low preference of fibroblasts to adhere to both hydrogels.

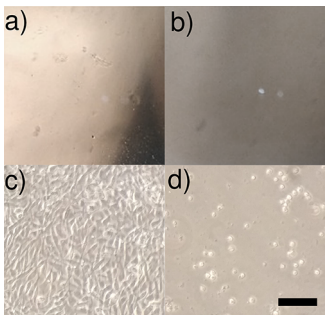

Figure 7. Microscopic pictures of NIH3T3 cells cultured on gum karaya/chitosan (GK/Ch) hydrogels with different ratios of GK and chitosan: (a) GK100/Ch0, (b) GK50/Ch50, (c) negative control for cytotoxicity (no hydrogel only NIH3T3 culture medium), (d) positive control for cytotoxicity (no hydrogel only NIH3T3 culture medium and SDS) (scale bar 1 mm).

However, NIH3T3 easily adhered to the empty wells containing the NIH3T3 culture medium (Figure 7c). Cells in control wells (positive control for cytotoxicity containing sodium dodecyl sulfate (SDS)) were detected, but in this case, most of the cells were dead or with a pathological round morphology due to the presence of toxic SDS (Figure 7d). These observations were similar at all three time points (24, 48, and 72 h; data not shown).

3.6. Mechanical Characterization of Hydrogel Films. To investigate the effect of composition, tensile strength tests were performed on all developed materials in the hydrated state to prove their applicability in wound dressing. The results of the tensile strength test in Figure 8 show that the elongation of the films is directly dependent on the hydrogel composition. PVA hydrogels generally form strong and tough polymer networks, and since there is a uniform PVA concentration, the effect of GK and chitosan is observed. The maximum mechanical performance in the breaking point range of 375.4 ± 18.8% shows sample GK100/Ch0 with applied stress of 3.5 ± 0.1 MPa and Young modulus ranging 3.2 ± 0.7 MPa. GK, together with PVA, form a strong, easily swellable, and elastic polymer network due to interactions of hydroxyl groups.

On the contrary, the poor mechanical performance of the films shows films with chitosan addition. The sample GK25/

Scheme 1. Proposed Mechanisms of Physical Crosslinking of Chitosan, GK, and PVA

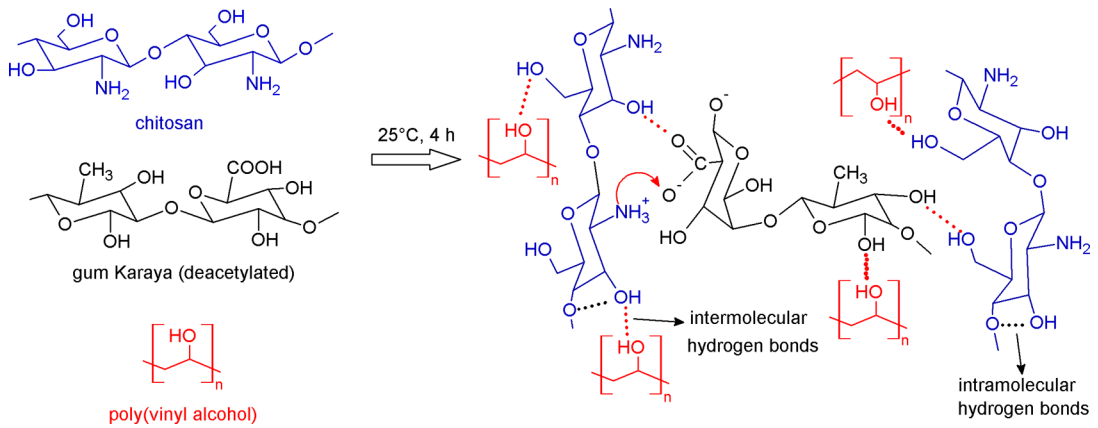

https://doi.org/10.1021/acsapm.3c00025
ACS Appl. Polym. Mater. 2023, 5, 2774−2786

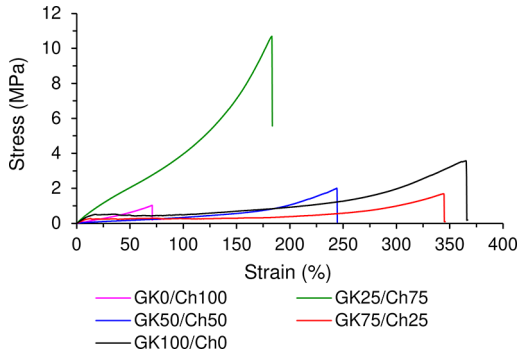

Figure 8. Average tensile strength (MPa) and the strain (%) at the breaking point of the gum karaya/chitosan (GK/Ch) hydrogel films with different ratios of GK and chitosan.

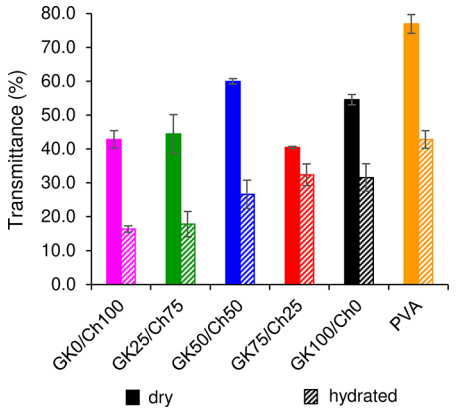

Figure 9. GK/Ch-based films' optical transparency at a wavelength of 600 nm with different compositions, as well as the films' state (dry/hydrated).

Ch75 was the most resistant to applied force, reaching applied stress in the range of 11.1 ± 1.3 MPa and Young modulus 4.6 ± 0.9 MPa at the breaking point with a maximum elongation of 195.8 ± 10.2%. This toughness is caused by forming a strong network composed of hydrogen−bond interactions between hydroxyl groups of GK, PVA, and chitosan, together with ionic interaction of GK carboxyl groups and chitosan amino groups. Moreover, the incompatible ratio between the polymers forms a more fragile network that possesses reduced resistance against applied stress. Samples with a lower chitosan addition GK75/Ch25 reach 2.5 ± 0.7 MPa, Young modulus 2.7 ± 0.8 MPa, and break point at 349.3 ± 12.7%; GK50/Ch50 has increased applied stress at the breaking point in the range of 2.3 ± 0.5 MPa with Young modulus 0.7 ± 0.2 MPa and maximum elongation of 261.3 ± 20.9%. The lowest values have sample GK0/Ch100 with applied stress of 1.3 ± 0.3 MPa, Young modulus 1.7 ± 0.5 MPa, and a breaking point ranging 74.4 ± 4.1% caused by the highly hydrophilic nature of the material with a less tough polymer network. Overall, the results proved that GK addition increases the film elasticity and mechanical strength of the gels almost linearly (Figure S2a in Supporting information) when hydrated, Figure 8 (x-axis). At the same time, tensile stress is influenced by the density of cross-linking between the polymers forming hydrogen and ionic bonds. A suitable ratio between components GK25 and Ch75 forms a rigid network. In contrast, the rest of the films possess three up to eight times lower resistance against applied stress (Figure S2b), which correlates with Young's modulus values of the material (Figure S3 in the Supporting information).

3.7. Optical Properties. Transparency is an essential feature of wound dressings since it allows wound visualization. Material transparency is dependent not only on the composition but also on the material's absorption of liquids (hydrophilicity). The material's optical transmittance (%T) spectra are shown in Figure S4a,b in the Supporting Information and represent the optical transmittance in the visible region.

Figure 9 compares the dry and hydrated state of all samples at a wavelength of 600 nm. All films' transparency has a similar trend with decreasing in transparency for the hydrated state. This fact is caused by the liquid absorption as the hydrogel matrix expands, and pore size enlarges as the material swells. The highest transparency is observed in pure PVA hydrogels that count 76.9 ± 1.6%T in the dry state and 42.8 ± 1.5%T in the wet state. The transparency of the GK/Ch hydrogel films in the dry state varies between 40 and 60%T at 600 nm with no observed composition dependency on the transparency.

On the contrary, the hydrated films show that composition strongly influences %T. Increasing transparency corresponds to a higher GK concentration caused by a strong hydrogel network with intermolecular hydrogen bonds. This trend can be correlated with a measurement of swelling behavior in which the films with the highest chitosan concentration (Figure 3) were the most hydrophilic (−OH and $-CH_2-OH$ groups), absorbing a large amount of water, resulting in pores enlargement decreasing transparency. The sample GK0/CH100 has transparency values in the range of 16.4 ± 0.6% T at 600 nm; compared to that, GK100/CH0 has twice higher transparency accounting for 31.6 ± 2.4%T. Overall, the films' wet state transparency with a range in values 16−32 decreased by about half compared to the dry state. Hydrogel transparency is strongly influenced by the film swelling behavior, which is directly proportional to the hydrogel composition. Gk/Ch-based hydrogel films have comparable transparency in the dry state with PVA-based hydrogels,[54] poly(methyl methacrylate) (PMMA),[55] or poly(2-hydroxyethyl methacrylate) (PHEMA) hydrogels,[56] which possess high transparency. Based on the results, we can conclude that GK/Ch-based hydrogel films possess sufficient transparency to monitor the wound site in the dry state, slightly decreasing when hydrated.

3.8. Cytotoxicity Test of Hydrogel Extracts on Adherent NIH3T3 Cells. To investigate the cytotoxicity of potentially released hydrogel compounds, adherent NIH3T3 fibroblasts were treated with hydrogel extracts. No morphological change or abnormal phenotype with changes in cell size and shape was detected after the incubation of both hydrogel extracts (GK100/Ch0, GK50/Ch50) with NIH3T3 cells (Figure S5a,b in the Supporting information) compared to the wells with the NIH3T3 culture medium (Figure S5c). Wells containing the cytotoxicity positive reference exhibited changes in cell size and shape (Figure S5d). Macroscopically, it was evident after Toluidine blue staining that the plates with SDS (cytotoxicity positive) were free of NIH3T3 cells after 24 and 72 h of exposure (Figure S5e). However, cells exposed to the negative control (complete cell culture medium) or hydrogel extracts (GK100/Ch0, GK50/Ch50) did not show visible acellular areas (Figure S5e−g). In total, we did not observe "zones of inhibition" of dead cells detached after PBS washing or any regions of the less dense cell layer compared to

https://doi.org/10.1021/acsapm.3c00025
ACS Appl. Polym. Mater. 2023, 5, 2774−2786

the blue-stained monolayer of the normal NIH3T3 population (negative control for cytotoxicity) after either 24 or 72 h of exposure (Figure S5f). The hydrogel extracts of GK100/Ch0 and GK50/Ch50 did not exhibit cytotoxic properties in adherent NIH3T3 cells (Figure S5g,h).

3.9. Cytotoxicity Test of Hydrogel Extracts on Suspension BaF3 Cells. After 24 h of exposure of the extracts to BaF3 cells, the difference between the SDS cytotoxic positive control and the hydrogel extracts was clear under the light microscope when the SDS control contained a lower number of cells compared to the other three conditions (BaF3 medium only, GK100/Ch0 extract, GK50/Ch50 extract). BaF3 cells are round suspension cells, and therefore, changes in cell morphology or the presence of an abnormal phenotype with changes in cell size and shape were not possible to evaluate. However, cells in all conditions after 24 h of exposure to the extracts were manually counted to three times per condition and the average number of all cells was calculated. The number of cells in a cytotoxicity-negative (BaF3 culture medium) plate was significantly higher (16×10^4 mL^{-1}) compared to the number of cells in the cytotoxicity-positive plate with SDS (6×10^4 mL^{-1}) ($^*P < 0.05$), representing approximately one-third of cells in the negative control plate (Figure 10a).

Cell counts from extracts of both hydrogels reached similar values as the reference (negative control for cytotoxicity), 16×10^4 mL^{-1} for GK100/Ch0 and 18×10^4 mL^{-1} for GK50/Ch50 (P = NS), representing 101 and 113% of cells in the negative plate, respectively (Figure 10a). Similarly, there was no difference between the live and dead cell compositions between the negative control and both hydrogel extracts (P = NS) (Figure 10b). As expected, there was a significant decrease in the number of live cells in the cytotoxicity positive control with SDS ($^{**}P < 0.01$) (Figure 10b). After 24 and 72 h of exposure, the metabolic activity of the BaF3 cells in each experimental condition (hydrogel extract, control references) was evaluated by the resazurin proliferation assay. Cell proliferation in both hydrogel extracts was increased compared to the negative control for cytotoxicity ($^{****}P < 0.0001$) (Figure 10c). On the other hand, there was a significant decrease in cell proliferation in the cytotoxicity positive control with SDS ($^{****}P < 0.0001$). No significant difference between 24 and 72 h of hydrogel exposure for any hydrogel extract was found. No detectable cytotoxic activities were observed either on the adherent NIH3T3 cells or the non-adherent suspension BaF3 cells. The graph shows the results of the fluorescence measurement (y-axis) of the metabolized resazurin that changed to fluorescent resorufin. Each bar represents the mean fluorescent value in arbitrary units (AU) with SD from three independent wells, each measured three times. $^{****}P < 0.0001$ (two-way ANOVA; using negative control as a reference). The studied hydrogels are slowly degradable, making them suitable for wound dressings that can be replaced every few days, depending on the type of wound. Thus, it is desirable that the newly formed tissue (containing fibroblasts) closing the wound would not adhere to the hydrogel as part of the dressing. Using different methods, our results demonstrated (i) no adherence of the fibroblasts NIH3T3 to the hydrogels and (ii) no detectable cytotoxic activity of our hydrogels' extracts on adherent cells (NIH3T3) or the non-adherent suspension cells (BaF3).

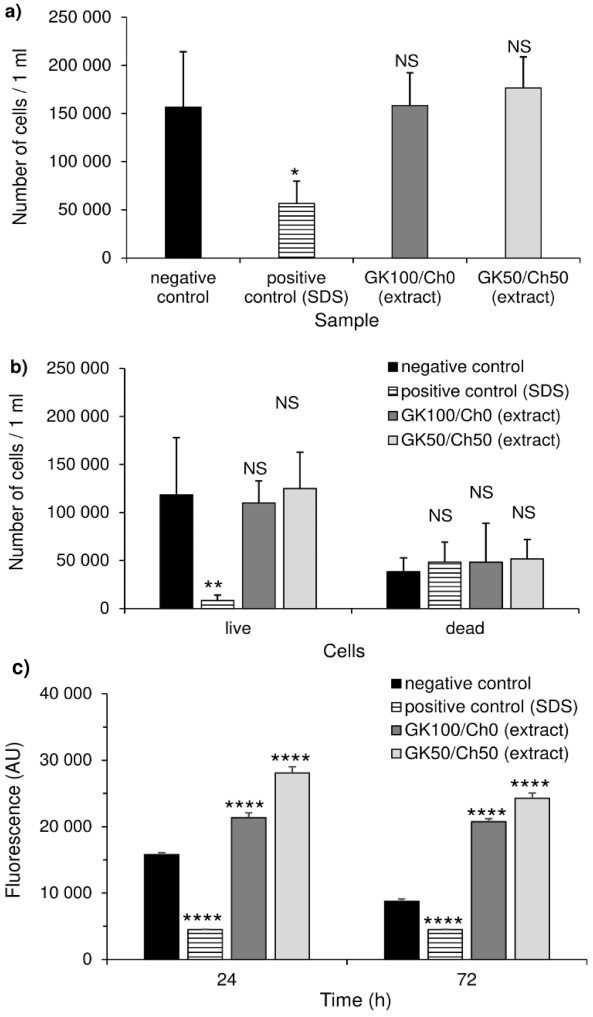

Figure 10. Cell counts of BaF3 cells exposed to various treatments on gum karaya/chitosan (GK/Ch) hydrogel extracts for 24 h. (a) All BaF3 cells (one-way ANOVA) and (b) composition of live and dead cells (two-way ANOVA) using negative control as a reference and SDS as a positive control. Each bar represents a mean cell count from three independent wells with a standard deviation (SD). $^*P < 0.05$; $^{**}P < 0.01$. (c) Proliferation activity of BaF3 cells exposed to various treatments on gum karaya/chitosan (GK/Ch) hydrogel extracts for 24 and 72 h measured by resazurin-based proliferation assay. Each bar represents mean fluorescence values from three independent wells with a standard deviation (SD). $^*P < 0.05$; $^{**}P < 0.01$, $^{**}P < 0.0001$.

4. CONCLUSIONS

The transparent hydrogel films from gum karaya and chitosan mixture were successfully prepared. Based on the type of the treated wound, the physicochemical properties can be tailored for a specific application. The ionic crosslinking between gum karaya and chitosan in acidic conditions (in the acute wound) allow the absorption of wound liquids (e.g., microbial effusion) and help to keep the wound clean and without microorganisms. The film's transparency in the wet state allows control of the healing process. Additionally, our combination of gum karaya and chitosan mixture exhibited synergistic antimicrobial activity against tested microbial strains, such as *Staphylococcus aureus*, *Pseudomonas aeruginosa*, and *Candida albicans*. Moreover, these hydrogels exhibited no cytotoxic effects on adherent as well as on suspension cells in in vitro experiments. There was no adhesion of fibroblast cells to the

https://doi.org/10.1021/acsapm.3c00025
ACS Appl. Polym. Mater. 2023, 5, 2774−2786

tested hydrogels suitable for non-adherent wound dressings. These hydrogels can also complement other promising approaches in wound care management, such as the development of antimicrobial nanoparticles or nanofibers, and even increase their beneficial effects. However, additional evaluation of their compatibility under physiological conditions should be investigated further using in vivo models. All of the described properties make these hydrogels unique and suitable for wound management and especially for the management of slow-healing and/or infected wounds. Due to the tailoring of the physicochemical properties, applications from short-term (in acute wounds) to long-term (in chronic wounds) use can be applied. Thanks to good mechanical properties, the manipulation and application are very easy and can be easily handled at hospitals or at home. The simple and cost-effective preparation of these hydrogels is potentially applicable on a pilot and industrial scale.

■ ASSOCIATED CONTENT

Supporting Information

The Supporting Information is available free of charge at https://pubs.acs.org/doi/10.1021/acsapm.3c00025.

Graphical illustration of the calculation of diffusion exponent n (slope) from the swelling behavior of gum karaya/chitosan (GK/Ch) blends with different ratios of gum karaya and chitosan; hydrogel's average strain at the breaking point and average elongation (strain) and the average applied stress at the breakpoint; Young's modulus of the hydrated GK/Ch hydrogel films; UV−vis transmittance spectra of the GK/Ch-based hydrogel films and pure PVA film in the dry and hydrated states; microscopic picture of NIH3T3 cells cultured in gum karaya/chitosan (GK/Ch) hydrogel extracts with different ratios of GK and chitosan after cytotoxic evaluation (PDF)

■ AUTHOR INFORMATION

Corresponding Author

Lucy Vojtová − *Central European Institute of Technology, Brno University of Technology, Brno 612 00, Czech Republic;* orcid.org/0000-0001-5281-7045; Email: lucy.vojtova@ceitec.vutbr.cz

Authors

Eva Drápalová − *Central European Institute of Technology, Brno University of Technology, Brno 612 00, Czech Republic*

Lenka Michlovská − *Central European Institute of Technology, Brno University of Technology, Brno 612 00, Czech Republic;* orcid.org/0000-0002-7963-1715

Hana Poštulková − *Central European Institute of Technology, Brno University of Technology, Brno 612 00, Czech Republic*

Ivana Chamradová − *Central European Institute of Technology, Brno University of Technology, Brno 612 00, Czech Republic;* orcid.org/0000-0001-7927-946X

Břetislav Lipový − *Central European Institute of Technology, Brno University of Technology, Brno 612 00, Czech Republic; Department of Burns and Plastic Surgery, Institution shared with University Hospital Brno, Faculty of Medicine, Masaryk University, Brno 625 00, Czech Republic*

Jakub Holoubek − *Department of Burns and Plastic Surgery, Institution shared with University Hospital Brno, Faculty of Medicine, Masaryk University, Brno 625 00, Czech Republic*

Lukáš Vacek − *Department of Microbiology, St. Anne's University Hospital Brno and Faculty of Medicine, Masaryk University, Brno 602 00, Czech Republic;* orcid.org/0000-0002-2045-2456

Filip Růžička − *Department of Microbiology, St. Anne's University Hospital Brno and Faculty of Medicine, Masaryk University, Brno 602 00, Czech Republic*

Markéta Hanslianová − *Department of Microbiology, St. Anne's University Hospital Brno and Faculty of Medicine, Masaryk University, Brno 602 00, Czech Republic; Department of Clinical Microbiology, University Hospital Brno, Brno 625 00, Czech Republic*

Táňa Svobodová − *Enantis, Brno 625 00, Czech Republic*

Eva Černá − *Central European Institute of Technology, Brno University of Technology, Brno 612 00, Czech Republic*

Barbara Hrdličková − *Enantis, Brno 625 00, Czech Republic*

Complete contact information is available at: https://pubs.acs.org/10.1021/acsapm.3c00025

Author Contributions

The manuscript was written through contributions of all authors. All authors have given approval to the final version of the manuscript.

Funding

This research was funded by the Ministry of Health of the Czech Republic under the grant number NU20-05-00166 and the Specific Research Project of the Brno University of Technology (grant number STI-J-17-4776). All rights reserved.

Notes

The authors declare no competing financial interest.

■ REFERENCES

(1) Stashak, T. S.; Farstvedt, E.; Othic, A. Update On Wound Dressings: Indications And Best Use. *Clin. Techn. Equine Practice* **2004**, *3*, 148−163.

(2) Wasiak, J.; Cleland, H.; Campbell, F.; Spinks, A.; Cochrane Wounds Group. Dressings For Superficial And Partial Thickness Burns. *Cochrane Database Syst. Rev.* **2013**, *2013*, No. CD002106.

(3) Üstündağ Okur, N.; Hökenek, N.; Okur, M. E.; Ayla, Ş.; Yoltaş, A.; Siafaka, P. I.; Cevher, E. An Alternative Approach To Wound Healing Field; New Composite Films From Natural Polymers For Mupirocin Dermal Delivery. *Saudi Pharmaceut J.* **2019**, *27*, 738−752.

(4) Lee, S. M.; Park, I. K.; Kim, Y. S.; Kim, H. J.; Moon, H.; Mueller, S.; Jeong, Y.-I. Physical, Morphological, And Wound Healing Properties Of A Polyurethane Foam-Film Dressing. *Biomater. Res* **2016**, *20*, 738−752.

(5) Essawy, A. A.; Hefni, H.; El-Nggar, A. M. Biocompatible And Biodegradable Chitosan Composites In Wound Healing Application: In Situ Novel Photo-Induced Skin Regeneration Approach. *Sustainable Polym. Compos. Nanocomposites* **2019**, *20*, 143−183.

(6) Kumar, A.; Kaur, H. Sprayed In-Situ Synthesis Of Polyvinyl Alcohol/Chitosan Loaded Silver Nanocomposite Hydrogel For Improved Antibacterial Effects. *Int. J. Biol. Macromol.* **2020**, *145*, 950−964.

(7) Mir, M.; Ali, M. N.; Barakullah, A.; Gulzar, A.; Arshad, M.; Fatima, S.; Asad, M. Synthetic Polymeric Biomaterials For Wound Healing: A Review. *Prog. Biomater.* **2018**, *7*, 1−21.

(8) Ponrasu, T.; Cheng, T. -H.; Wang, L.; Cheng, Y. -S.; Wang, H. -M. D. Natural Biocompatible Polymer-Based Polyherbal Compound Gel For Rapid Wound Contraction And Promote Re-Epithelialization: An In Vivo Study. *Mater. Lett.* **2020**, *261*, 217−233.

(9) Ghadi, R.; Jain, A.; Khan, W.; Domb, A. J. Microparticulate Polymers And Hydrogels For Wound Healing. *Wound Heal. Biomater.* **2016**, 203−225.

(10) Singh, B.; Pal, L. Development Of Sterculia Gum Based Wound Dressings For Use In Drug Delivery. *Eur. Polym. J.* **2008**, *44*, 3222−3230.
(11) Kamoun, E. A.; Chen, X.; Mohy Eldin, M. S.; Kenawy, E. -R. S. Crosslinked Poly(Vinyl Alcohol) Hydrogels For Wound Dressing Applications: A Review Of Remarkably Blended Polymers. *Arab. J. Chem.* **2015**, *8*, 1−14.
(12) Kamoun, E. A.; Kenawy, E. -R. S.; Chen, X. A Review On Polymeric Hydrogel Membranes For Wound Dressing Applications: Pva-Based Hydrogel Dressings. *J. Adv. Res.* **2017**, *8*, 217−233.
(13) Olewnik-Kruszkowska, E.; Gierszewska, M.; Jakubowska, E.; Tarach, I.; Sedlarik, V.; Pummerova, M. Antibacterial Films Based On Pva And Pva−Chitosan Modified With Poly(Hexamethylene Guanidine). *Polymer* **2019**, *11*, 2093.
(14) Singh, B.; Pal, L. Sterculia Crosslinked Pva And Pva-Poly(Aam) Hydrogel Wound Dressings For Slow Drug Delivery: Mechanical, Mucoadhesive, Biocompatible And Permeability Properties. *J. Mech. Behav. Biomed Mater.* **2012**, *9*, 9−21.
(15) Singh, B.; Vashishtha, M. Development Of Novel Hydrogels By Modification Of Sterculia Gum Through Radiation Cross-Linking Polymerization For Use In Drug Delivery. *Nucl Instrum Methods Phys Res B NUCL INSTRUM METH B* **2008**, *266*, 2009−2020.
(16) Chandel, A. K. S.; Bera, A.; Nutan, B.; Jewrajka, S. K. Reactive Compatibilizer Mediated Precise Synthesis And Application Of Stimuli Responsive Polysaccharides-Polycaprolactone Amphiphilic Co-Network Gels. *Polymer* **2016**, *99*, 470−479.
(17) Fraser, J. F.; Cuttle, L.; Kempf, M.; Kimble, R. M. Cytotoxicity Of Topical Antimicrobial Agents Used In Burn Wounds In Australasia. *ANZ J. Surg* **2004**, *74*, 139−142.
(18) Mihai, M. M.; Dima, M. B.; Dima, B.; Holban, A. M. Nanomaterials For Wound Healing And Infection Control. *Materials* **2019**, *12*, 139−142.
(19) Bahulkar, S. S.; Munot, N. M.; Surwase, S. S. Synthesis, Characterization Of Thiolated Karaya Gum And Evaluation Of Effect Of Ph On Its Mucoadhesive And Sustained Release Properties. *Carbohydr. Polym.* **2015**, *130*, 183−190.
(20) Postulkova, H.; Chamradova, I.; Pavlinak, D.; Humpa, O.; Jancar, J.; Vojtova, L. Study Of Effects And Conditions On The Solubility Of Natural Polysaccharide Gum Karaya. *Food Hydrocolloids* **2017**, *67*, 148−156.
(21) Vellora Thekkae Padil, V.; Nguyen, N. H. A.; Ševců, A.; Černík, M. Fabrication, Characterization, And Antibacterial Properties Of Electrospun Membrane Composed Of Gum Karaya, Polyvinyl Alcohol, And Silver Nanoparticles. *J. Nanomater.* **2015**, *2015*, 1−10.
(22) Raj, V.; Lee, J.-H.; Shim, J.-J.; Lee, J. Recent Findings And Future Directions Of Grafted Gum Karaya Polysaccharides And Their Various Applications: A Review. *Carbohydr. Polym.* **2021**, *258*, 117687.
(23) Leonhardt, E. E.; Kang, N.; Hamad, M. A.; Wooley, K. L.; Elsabahy, M. Absorbable Hemostatic Hydrogels Comprising Composites Of Sacrificial Templates And Honeycomb-Like Nanofibrous Mats Of Chitosan. *Nat. Commun.* **2019**, *10*, 235−240.
(24) Alven, S.; Aderibigbe, B. A. Chitosan And Cellulose-Based Hydrogels For Wound Management. *Int. J. Mol. Sci.* **2020**, *21*, 9656.
(25) Shojaee Kang Sofla, M.; Mortazavi, S.; Seyfi, J. Preparation And Characterization Of Polyvinyl Alcohol/Chitosan Blends Plasticized And Compatibilized By Glycerol/Polyethylene Glycol. *Carbohydr. Polym.* **2020**, *232*, 115784.
(26) Yang, W.; Fortunati, E.; Bertoglio, F.; Owczarek, J. S.; Bruni, G.; Kozanecki, M.; Kenny, J. M.; Torre, L.; Visai, L.; Puglia, D. Polyvinyl Alcohol/Chitosan Hydrogels With Enhanced Antioxidant And Antibacterial Properties Induced By Lignin Nanoparticles. *Carbohydr. Polym.* **2018**, *181*, 275−284.
(27) Warmuth, M.; Kim, S.; Gu, X.; Xia, G.; Adrián, F. Ba/F3 Cells And Their Use In Kinase Drug Discovery. *Curr. Opin. Oncol.* **2007**, *19*, 55−60.
(28) Lipový, B.; Holoubek, J.; Vacek, L.; Růžička, F.; Nedomová, E.; Poštulková, H.; Vojtová, L. Antimicrobial Effect Of Novel Hydrogel Matrix Based On Natural Polysaccharide Sterculia Urens. *Epidemiol. Mikrobiol. Imunol* **2018**, *67*, 166−174.
(29) Dorazilová, J.; Muchová, J.; Šmerková, K.; Kočiová, S.; Diviš, P.; Kopel, P.; Veselý, R.; Pavliňáková, V.; Adam, V.; Vojtová, L. Synergistic Effect Of Chitosan And Selenium Nanoparticles On Biodegradation And Antibacterial Properties Of Collagenous Scaffolds Designed For Infected Burn Wounds. *Nanomaterials* **2020**, *10*, 1971.
(30) Fu, Y.; Kao, W. J. Drug Release Kinetics And Transport Mechanisms Of Non-Degradable And Degradable Polymeric Delivery Systems. *Expert Opin Drug Delivery* **2010**, *7*, 429−444.
(31) Vojtová, L.; Pavliňáková, V.; Muchová, J.; Kacvinská, K.; Brtníková, J.; Knoz, M.; Lipový, B.; Faldyna, M.; Göpfert, E.; Holoubek, J.; Pavlovský, Z.; Vícenová, M.; Blahnová, V.; Hearnden, V.; Filová, E. Healing And Angiogenic Properties Of Collagen/Chitosan Scaffolds Enriched With Hyperstable Fgf2-Stab® Protein: In Vitro, Ex Ovo And In Vivo Comprehensive Evaluation. *Biomedicines* **2021**, *9*, 590.
(32) Nayak, A. K.; Hasnain, M. S.; Nayak, A. K.; Hasnain, M. S. Sterculia Gum Based Multiple Units For Oral Drug Delivery. *Plant Polysaccharides-Based Multiple-Unit Systems for Oral Drug Delivery* **2019**, 67−82.
(33) Sahariah, P.; Másson, M. Antimicrobial Chitosan And Chitosan Derivatives: A Review Of The Structure−Activity Relationship. *Biomacromolecules* **2017**, *18*, 3846−3868.
(34) Goy, R. C.; de Britto, D.; Assis, O. B. G. A Review Of The Antimicrobial Activity Of Chitosan. *Polímeros* **2009**, *19*, 241−247.
(35) Ke, C.-L.; Deng, F.-S.; Chuang, C.-Y.; Lin, C.-H. Antimicrobial Actions And Applications Of Chitosan. *Polymer* **2021**, *13*, 904−925.
(36) Guarnieri, A.; Triunfo, M.; Scieuzo, C.; et al. Antimicrobial properties of chitosan from different developmental stages of the bioconverter insect *Hermetia illucens*. *Sci. Rep.* **2022**, *12*, 8084.
(37) Ferraris, S.; Örlygsson, G.; Ng, C. H.; Riccucci, G.; Spriano, S. Chemical, Physical, And Mechanical Characterization Of Chitosan Coatings On A Chemically Pre-Treated Ti6Al4V Alloy. *Surf. Coat. Technol.* **2022**, *441*, 128571.
(38) Li, X.; Shang, L.; Li, D.; Wang, W.; Chen, S.; Zhong, H.; Huang, Y.; Long, S. l Polyelectrolyte Complex Hydrogel Films From Natural Polysaccharides. *Polym. Test.* **2022**, *109*, 107547.
(39) Hajji, S.; Chaker, A.; Jridi, M.; Maalej, H.; Jellouli, K.; Boufi, S.; Nasri, M. Structural Analysis, And Antioxidant And Antibacterial Properties Of Chitosan-Poly (Vinyl Alcohol) Biodegradable Films. *Environ. Sci. Pollut. Res.* **2016**, *23*, 15310−15320.
(40) Lawrie, G.; Keen, I.; Drew, B.; Chandler-Temple, A.; Rintoul, L.; Fredericks, P.; Grøndahl, L. Interactions Between Alginate And Chitosan Biopolymers Characterized Using Ftir And Xps. *Biomacromolecules* **2007**, *8*, 2533−2541.
(41) Singh, B.; Chauhan, G. S.; Sharma, D. K.; Kant, A.; Gupta, I.; Chauhan, N. The Release Dynamics Of Model Drugs From The Psyllium And N-Hydroxymethylacrylamide Based Hydrogels. *Int. J. Pharm.* **2006**, *325*, 15−25.
(42) Dash, S.; Murthy, P. N.; Nath, L.; Chowdhury, P. Kinetic Modeling On Drug Release From Controlled Drug Delivery Systems. *Acta Poloniae Pharmaceut.* **2010**, *67*, 217−223.
(43) Zarzycki, R.; Modrzejewska, Z.; Nawrotek, K. Drug Release From Hydrogel Matrices. *Ecol. Chem. Eng. S* **2010**, *17*, 118−136.
(44) Caccavo, D.; Cascone, S.; Lamberti, G.; Barba, A. A.; Larsson, A. Swellable Hydrogel-Based Systems For Controlled Drug Delivery. *Smart Drug Deliv Syst* **2016**, DOI: 10.5772/61792.
(45) Ono, S.; Imai, R.; Ida, Y.; Shibata, D.; Komiya, T.; Matsumura, H. Increased Wound Ph As An Indicator Of Local Wound Infection In Second Degree Burns. *Burns* **2015**, *41*, 820−824.
(46) Qu, X.; Wirsén, A.; Albertsson, A.-C. Novel Ph-Sensitive Chitosan Hydrogels: Swelling Behavior And States Of Water. *Polymer* **2000**, *41*, 4589−4598.
(47) Szymańska, E.; Winnicka, K. Stability Of Chitosan—A Challenge For Pharmaceutical And Biomedical Applications. *Marine Drugs* **2015**, *13*, 1819−1846.

(48) Sadeghi, M. Synthesis And Swelling Behaviors Of Graftcopolymer Based On Chitosan-G-Poly(Aa-Co-Hema). *Int. J. Chem Eng. App.* **2010**, *1*, 354−358.
(49) Nugraheni, A. D.; Purnawati, D.; Rohmatillah, A.; Mahardika, D. N.; Kusumaatmaja, A. Swelling Of Pva/Chitosan/Tio₂ Nanofibers Membrane In Different Ph. *Mater. Sci. Forum* **2020**, *990*, 220−224.
(50) Watters, C.; Yuan, T. T.; Rumbaugh, K. P. Beneficial And Deleterious Bacterial−Host Interactions In Chronic Wound Pathophysiology. *Chronic Wound Care Manag. Res.* **2015**, *2*, 53−62.
(51) Peppas, N. A.; Khare, A. R. Preparation, Structure And Diffusional Behavior Of Hydrogels In Controlled Release. *Adv. Drug Delivery Rev.* **1993**, *11*, 1−35.
(52) Sazegar, M.; Bazgir, S.; Katbab, A. A. Preparation And Characterization Of Water-Absorbing Gas-Assisted Electrospun Nanofibers Based On Poly(Vinyl Alcohol)/Chitosan. *Mater. Today Commun.* **2020**, *25*, 101489.
(53) Ramakrishnan, R. K.; Padil, V. V. T.; Wacławek, S.; Černík, M.; Varma, R. S. Eco-Friendly And Economic, Adsorptive Removal Of Cationic And Anionic Dyes By Bio-Based Karaya Gum—Chitosan Sponge. *Polymer* **2021**, *13*, 251.
(54) Guo, M.; Yan, J.; Yang, X.; Lai, J.; An, P.; Wu, Y.; Li, Z.; Lei, W.; Smith, A. T.; Sun, L. A Transparent Glycerol-Hydrogel With Stimuli-Responsive Actuation Induced Unexpectedly At Subzero Temperatures. *J. Mater. Chem. A* **2021**, *9*, 7935−7945.
(55) Choi, J. -W.; Lee, J. H. Selectively Uv-Blocking And Visibly Transparent Adhesive Films Embedded With Tio2/Pmma Hybrid Nanoparticles For Displays. *Materials* **2020**, *13*, 5273.
(56) Mutar, M. A. Synthesis And Biocompatibility Of New Contact Lenses Based On Derivatives Of 2-Hydroxy Ethyl Meth Acrylate And 2-Ethyl Hexyl Methacrylate. *Int. J. Res. Studies Biosci.* **2015**, *3*, 1−9.

https://doi.org/10.1021/acsapm.3c00025
ACS Appl. Polym. Mater. 2023, 5, 2774−2786